Available online at www.sciencedirect.com
ScienceDirect
Applied Catalysis A: General 334 (2008) 156–167
APPLIED CATALYSIS A: GENERAL
www.elsevier.com/locate/apcata

Hydrodechlorination of CCl_4 over Pt/γ-Al_2O_3 prepared from different Pt precursors

Jong Wook Bae [a,*], Jae Sung Lee [b], Kyung Hee Lee [b]

[a] *Advanced Chemical Technology Division, Korea Research Institute of Chemical Technology (KRICT), P.O. Box 107, Yuseong, Daejeon 305-343, South Korea*

[b] *Department of Chemical Engineering and School of Environmental Engineering, Pohang University of Science and Technology (POSTECH), San 31, Hyoja-dong, Pohang 790-784, South Korea*

Received 25 April 2007; received in revised form 5 September 2007; accepted 1 October 2007
Available online 5 October 2007

Abstract

The platinum particle size on γ-Al_2O_3 prepared from different platinum precursors such as $Pt(NH_3)_2(NO_2)_2$, H_2PtCl_6, and K_2PtCl_6, and its effect on hydrodechlorination (HDC) of CCl_4 with the variation of calcination temperatures was investigated. It concomitantly affects the products distribution and catalytic stability in HDC of CCl_4. To verify the effects of platinum particle size with different platinum precursors on the product distribution, the catalysts have been characterized by HRTEM and CO chemisorption, FT-IR, and TP methods (TPR, TPD and TPSR). The catalysts with small platinum particles, which possess low coordination number and electron-deficient character, favor the complete dechlorination of CCl_4 and produce CH_4 more selectively. It could be due to the strong adsorption strength of CCl_4 or the decreased activation energy of surface intermediates on small platinum particles. FT-IR studies reveal that the maximum peak position of linear-bonded CO shifted to the higher frequency with the increase of platinum particle size in all catalysts prepared from three different platinum precursors. While the selectivity to CH_4 increased with the decrease in the platinum particle size, the total amount of carbonaceous species on the platinum particles was enhanced. The larger the platinum particle, the higher the selectivity to $CHCl_3$ was obtained in all tested catalysts under the non-deactivating condition.

Keywords: Hydrodechlorination; CCl_4; Platinum particle size; γ-Al_2O_3; Product distribution

1. Introduction

Chlorinated organic compounds, including CCl_4, are known as one of the most hazardous ozone-depleting compounds with high carcinogenic activity and toxicity. The catalytic hydrodechlorination (HDC) is a promising technology to transform them into more useful, but less harmful hydrochloro-products [1–9]. Supported noble metals are usually employed as catalysts for HDC process. In general, to achieve a high catalytic activity with a small amount of expensive noble metal, various methods were reported to obtain high metal dispersions [10–17]. The metals are sometimes based on the formation of more facile mobile metal oxides or oxychlorides. Different preparation methods may also induce the difference in morphology and size distribution of metal particles. In HDC reaction, however, it has been suggested that the small metal particles are easily deactivated by strongly adsorbed chlorine [6,18–20] or enhanced coke deposition [7,21,22]. It was reported that the selectivity and catalyst stability were enhanced on the large particles over Pt/Al_2O_3-containing surface metal atoms with large coordination numbers [6,9,10,22], which could be related with the weak adsorption strength of surface intermediates in HDC of CCl_4. Zhang and Beard [6,10] have shown that durability of Pt/Al_2O_3 catalyst in HDC of CCl_4 was strongly dependent on the platinum particle size. The catalyst stability increased dramatically as the platinum particle size was increased to above 5–8 nm by NH_4Cl treatment followed by reduction. The large platinum particle, like a bulk platinum metal, exhibited a strong resistance to chloride poisoning and showed a longer catalyst life in HDC of CCl_4. In our previous work on HDC of CCl_4 [5,15,22], the product distribution was markedly affected by the oxidation states of platinum on γ-Al_2O_3, which was characterized by X-ray absorption near edge structure (XANES) white line areas.

* Corresponding author. Tel.: +82 42 860 7383; fax: +82 42 860 7388.
E-mail address: finejw@krict.re.kr (J.W. Bae).

0926-860X/$ – see front matter
doi:10.1016/j.apcata.2007.10.001

An optimum oxidation state of platinum particles existed that showed the best selectivity to $CHCl_3$. Platinum particles in the higher or lower oxidation states that the optimum value could promote the formation of CH_4 and C_2 oligomers.

Many researchers have investigated to show the effects of catalyst particle size on catalytic activity and selectivity and to correlate them with characterization results of XAFS, XPS, TEM, FT-IR, and coke analysis [4,8,10,22–36]. These effects are often accounted in terms of electronic and/or geometric effects. But, in many cases, geometric and electronic effects cannot be separated as independent variables. Furthermore, with the thermal treatment of Pt/Al_2O_3 above 800 °C, reduction of BET surface area, transformation of alumina phase and platinum particles agglomeration concomitantly occurs [26] resulting in changes in the catalytic activity. Noble metal particles formed on common oxide supports such as alumina or silica are often electron-deficient. The electron-deficient character of metal particle is stronger for smaller particles due to intrinsic size effects [32] or a strong metal support interaction upon high temperature reduction. The latter effect could be caused by a charge transfer between the metal particles and support or by other local interaction between them. The electronic state of supported metal particles is often probed by the infrared spectroscopy of CO adsorbed on them. In general, CO molecule could be coordinatively adsorbed on the metal atom through the 5σ orbital and the d orbital of transition metal atom backdonating charge to the $2\pi^*$ orbital of CO. Thus it weakens the C–O bond resulted in shifting the CO absorption bands to lower frequencies. For example, in the *n*-hexane conversion to benzene over zeolite-supported platinum catalysts, some authors have shown that the benzene selectivity increases with the shift of linear-bonded CO bands to lower frequencies indicating an increase in the electron density of the surface metal atoms. It was also related with the distribution and morphology of platinum particles in the pore of zeolite [23,24]. Kappers and van der Maas have shown a correlation between the frequency of linear-bonded CO and the platinum coordination number, i.e., the frequency of the stretching bands of linear-bonded CO increased with the increasing metal particle size [25]. In oxychlorination over Pt/Al_2O_3 catalyst, Mordente and Rochester [13] found that the best dispersion of platinum metals occurred for the reduced platinum atoms strongly interacting with the alumina support. They showed that the band at 2074 cm^{-1} resulted from the linear-bonded CO on the platinum arrays or mats strongly interacting with the alumina support, and the band at 2052 cm^{-1} was assigned to the adsorbed CO on sintered platinum particles with a high level of coordinative unsaturation. Greenler et al. [31] showed the correlation between the shift of linear-bonded CO frequencies and platinum morphology in the stepped single-crystal surfaces: a (1 1 1) crystal; a crystal with (1 1 1) terraces and (1 0 0) steps; a crystal with (1 1 1) terraces and kinked steps. The frequency of CO bands associated with terrace sites appeared at about 2085 cm^{-1} and that with step and kink sites at about 2065 cm^{-1}.

Furthermore, small platinum particles are generally in the state of electron deficiency owing to the strong interaction with Lewis acid sites of the support or their intrinsic electronic character. Surface carbons including surface carbide and amorphous or graphitic carbon formed during the reaction show a different temperature to be taken off [32,33]. The deposited hydrocarbons might also affect work function of metal by donating electron from the adsorbed hydrocarbon to supported platinum particles [34]. To certify the sort of surface carbon at steady-state conditions, temperature-programmed surface reaction (TPSR) and FT-IR were carried out. The general rule is that the more unsaturated the molecule, the more it is favorable to form strongly adsorbed species. In our reaction conditions [7], C_2Cl_4, major by-product, had much stronger adsorption capacity on platinum surfaces. Furthermore, CCl_4 showing electron-donating character could induce much stronger interaction with small platinum particle [5,7]. In addition, some authors identified the FT-IR peaks of the adsorbed hydro- or chlorohydrocarbons, including the chlorinated ethylenes, CH_2Cl_2, and butanes. These molecules showed the characteristic peak position of carboxylate- or acetate-type species and C–H bending modes and it was discussed below in detail [35–37].

To the best of our knowledge, the present study focused on showing the correlation between product distribution and the platinum particle size according to platinum precursors employed for the catalyst preparation in HDC of CCl_4 over a supported platinum catalyst (0.5 wt.% Pt/γ-Al_2O_3). The size of platinum particle was varied with changing oxidation temperature with three different types of catalysts between 373 and 1073 K, and it affected the selectivity to $CHCl_3$ in HDC reaction of CCl_4 due to the different electronic states of platinum particles on γ-Al_2O_3 support. The large platinum particles generally favor the high selectivity to $CHCl_3$ over supported platinum catalyst. It was also shown through the characterization methods with FT-IR of adsorbed CO, HRTEM, and CO chemisorption method for platinum particle size and TPD of CCl_4, TPSR, and FT-IR for carbonaceous species related with the adsorption strength of reaction intermediates.

2. Experimental

2.1. Catalyst preparation and activity measurements

The 0.5 wt.% Pt catalysts supported on γ-Al_2O_3 were prepared from different platinum precursors; 3.4 wt.% $Pt(NH_3)_2(NO_2)_2$ in dilute ammonium hydroxide solution, 8 wt.% H_2PtCl_6 in water and K_2PtCl_6 supplied by Aldrich. The support in the form of extruded pellets was provided by Strem and had a BET surface area of 103.5 m^2/g and pore volume of 0.5 cm^3/g. The pellet was crushed to form a powder with the size of 20–50 mesh (0.289–0.841 mm) and was used for preparing the catalyst by the conventional wet impregnation method. The solution of platinum precursors and the crushed support were mixed together and stirred in 100 ml distilled water over 12 h in a rotary evaporator. The catalyst was dried at 380 K for 24 h in an oven. The prepared catalysts were calcined at different temperatures ranging from 373 to 1073 K in an

Table 1
Pretreatment conditions of 0.5 wt.% Pt/γ-Al_2O_3 and platinum particle size characterized by CO chemisorption

Platinum precursor	Catalysts (notation)	Pretreatment conditions	Dispersion (%)	Particle size (nm)
$Pt(NH_3)_2(NO_2)_2$	PtN373	Dried at 373 K	34.6	2.59
	PtN573	Calcined at 573 K	98.2	0.91
	PtN773	Calcined at 773 K	52.8	1.70
	PtN1073	Calcined at 1073 K	7.78	11.5
H_2PtCl_6	PtH373	Dried at 373 K	57.6	1.55
	PtH573	Calcined at 573 K	74.7	1.20
	PtH773	Calcined at 773 K	23.6	3.80
	PtH1073	Calcined at 1073 K	5.94	15.1
K_2PtCl_6	PtK373	Dried at 373 K	42.6	2.10
	PtK573	Calcined at 573 K	49.6	1.81
	PtK773	Calcined at 773 K	14.0	6.41
	PtK1073	Calcined at 1073 K	–	–

Platinum dispersion and particle size were calculated from the amount of chemisorbed CO with the assumption that the ratio of adsorbed CO molecules on surface platinum atoms were close to 1.0, and that the particles were in a spherical shape.

airflow of 42.2 μmol/s. As shown in Table 1, the catalysts are denoted by a code system to identify their precursor and calcination temperatures. N stands for $Pt(NH_3)_2(NO_2)_2$, H for H_2PtCl_6, K for K_2PtCl_6 and the following digits for calcination temperatures. Thus, PtN573 represents the catalyst prepared from $Pt(NH_3)_2(NO_2)_2$ with a calcination temperature of 573 K. After in situ reduction with a H_2 flow (52 μmol/s) at 573 K for 3 h in a stainless steel micro-reactor (12.7 mm O.D.) with 0.5 g catalyst, the reaction temperature and pressure were adjusted to the desired values. The CCl_4 reactant with a purity higher than 99.9% (Aldrich) was used and hydrogen gas with a purity over 99.995% were used after passing through a molecular sieve trap (Alltech) to remove water. A feed of hydrogen was controlled to maintain a constant mole ratio of H_2/CCl_4 by a mass-flow controller (Brooks). The liquid CCl_4 was introduced by liquid pump to a mixing chamber, which was maintained at around 400 K. Effluent gases were analyzed by a HP 6890 gas chromatograph equipped with a HP-5 capillary column (30 m × 0.32 mm i.d., Hewlett Packard) and a flame ionization detector.

2.2. Characterization

2.2.1. CO chemisorption and HRTEM studies

To characterize the platinum particle size on γ-Al_2O_3, CO chemisorption was carried out at room temperature (RT) on catalyst (0.5 g) reduced in situ at 573 K for 3 h. In a static volumetric adsorption apparatus equipped with a high-vacuum pump providing vacuum in the order of 10^{-6} Torr, two successive isotherms separated by evacuation were obtained at RT. The difference of the two isotherms extrapolated to zero pressure was considered the amount of chemisorbed CO. The dispersion (D; % platinum exposed on the surface) and particle size (d_p) of platinum were calculated from the amount of chemisorbed CO assuming an adsorption stoichiometry (CO/Pt) of unity and spherical platinum particles. High-resolution transmission electron microscopy (HRTEM) experiment was carried out with a TECNAI G^2 instrument accelerated at 200 kV.

2.2.2. Temperature-programmed methods (TPR, TPSR, and TPD)

To carry out temperature-programmed reduction (TPR) using a thermal conductivity detector (TCD) cell, the prepared catalyst (0.5 g) was loaded in a quartz reactor and purged with a flow of He at 573 K for 1 h. It was heated at a linear ramping rate of 10 K/min from 323 to 1073 K with a flow of 5% H_2 balanced with N_2 (41 μmol/s). The temperature was adjusted in an electric furnace controlled by a PID controller and a local thermocouple contacting the sample powders. The effluent gases were sent to the TCD cell followed by passing through the molecular sieve trap that was kept at ice water thermostat to remove the generated water. In order to characterize the amount and the nature of deposited carbonaceous species, temperature-programmed surface reaction (TPSR) was performed by using the catalyst which was prepared at the following reaction conditions showing a stable activity: reduction $T = 573$ K; $T = 413$ K for 5 h; mole ratio of $H_2/CCl_4 = 25$; WHSV = 4500 l/(kg h) with 0.2 g catalyst. After purging with H_2 flow at 323 K for 3 h, gaseous products, CH_4 ($m/z = 16$) and C_2H_6 ($m/z = 28$), were analyzed continuously by a mass selective detector (HP-MSD 5973) while the sample temperature was raised linearly at a ramping rate of 10 K/min with H_2 gas (20.5 μmol/s). To carry out the temperature-programmed desorption (TPD) of CCl_4, the prepared catalyst (0.3 g) was reduced in H_2 flow (20.5 μmol/s) at 573 K for 3 h in a quartz reactor, and purged with He at 673 K for 1 h. CCl_4 was introduced onto the reduced catalyst at 323 K for 0.5 h by passing He carrier gas (He/CCl_4 mole ratio of 25) through a saturator-containing CCl_4. The temperature of the saturator was controlled by a circulating bath to adjust the He/CCl_4 mole ratio. TPD analysis was conducted in a desired temperature range after purging with He for more than 2 h to remove physisorbed CCl_4.

2.2.3. FT-IR studies for adsorbed CO and the carbonaceous species

FT-IR experiments of adsorbed CO were conducted using a thin pellet (diameter of ca. 10 mm) previously prepared by

pressing the pretreated catalyst (12 ± 1.0 mg) and loaded in an infrared cell equipped with CaF_2 windows. The thin pellet was reduced in situ under H_2 flow (20.5 μmol/s) at 573 K for 2 h and cooled to RT. After CO gas was introduced, the cell was equilibrated at atmospheric pressure (P_{CO} = 760 Torr) and RT, it was then evacuated for 30 min at the same temperature. Transmission infrared spectra of chemisorbed CO were collected using a Perkin-Elmer 1000 Fourier transform infrared (FT-IR) spectrometer. In order to obtain the infrared spectra of carbonaceous species in used catalysts, a pellet of the prepared catalyst was subjected to the pretreatment and HDC of CCl_4 under the same conditions employed in the TPSR experiments. After evacuating the samples at 10^{-6} Torr for 1 h at RT, FT-IR spectra were recorded.

3. Results

The product distribution of HDC of CCl_4 was varied to a great extent with reaction temperatures as shown in Fig. 1. The selectivity of $CHCl_3$ decreased while that of CH_4 increased with the reaction temperature. Furthermore, the generation of CH_2Cl_2 was also enhanced monotonically by increasing the reaction temperature. At a fixed reaction temperature, however, the mole ratio of $CHCl_3/CH_4$ remained almost constant with a variation of contact time (not shown). This implies that the HDC of CCl_4 over Pt/γ-Al_2O_3 could produce $CHCl_3$ and CH_4 on different reaction sites or by a parallel reaction pathway, as proposed earlier by Weiss et al. [1].

3.1. Changes in platinum particle size and FT-IR spectra of adsorbed CO

To investigate the effect of the platinum particle size, 0.5 wt.% Pt/γ-Al_2O_3 catalysts prepared from different platinum precursors such as $Pt(NH_3)_2(NO_2)_2$, H_2PtCl_6, and K_2PtCl_6, and were calcined at different temperatures. The pretreatment conditions are noted in Table 1. The platinum particle size determined by CO chemisorption was confirmed by HRTEM images, as shown in Table 1 and Fig. 2. The catalysts prepared from different platinum precursors by direct reduction and without calcinations (Pt373 groups) produced larger platinum particles on γ-Al_2O_3 compared to the catalysts calcined at 573 K prior to reduction (Pt573 groups). Above the clcination temperature of 573 K, small platinum particles agglomerated by the well-known sintering process by possibly forming a mobile platinum oxides or oxychloride species [10–17]. Thus, it appears that calcinations induce redispersion of platinum particle below 573 K, but undergoes sintering at much higher temperatures. The sintering process was more facile on the catalysts prepared from chloride-containing precursors (H_2PtCl_6 and K_2PtCl_6), probably due to the formation of volatile oxychloride species.

As shown in HRTEM images of Fig. 2, platinum particles formed in the catalysts prepared from $Pt(NH_3)_2(NO_2)_2$ precursor without calcinations (PtN373) were in the size of below 1 nm to around 5 nm (Fig. 2a). The large platinum particles in PtN373 were redispersed at the calcination temperature of 573 K, but the small platinum particles especially below 1 nm sintered and disappeared after calcination at 773 K. Although the platinum particle size in PtN373 showed a bi-modal size distribution, it was well dispersed in the chlorine-containing PtH373 and PtK373 catalysts (Fig. 2b and c). The FT-IR spectra shown in Fig. 3 reveals that the adsorbed CO on platinum particles was in the form of linear-bonded CO at the frequency of 2068–2094 cm^{-1}, and no bridged CO was detected. The frequency of linear-bonded CO shifted to higher frequencies with the increase of platinum particle size in all catalysts studied. The peak intensity of adsorbed CO molecule followed the similar trend of adsorbed CO measured from platinum dispersion (Table 1). The shift to the lower frequency in FT-IR could be related with the electronic states of platinum particles and the adsorption strength of reactants.

3.2. Temperature-programmed reduction (TPR)

Temperature-programmed reduction (TPR) profiles of the catalysts are shown in Fig. 4. The results suggest that the amount of hydrogen consumption of pre-oxidized catalysts prepared from $Pt(NH_3)_2(NO_2)_2$ and H_2PtCl_6 precursors was diminished with increasing the calcination temperature and the catalysts were almost reduced below 573 K. The amount of platinum oxides could increase with increasing the oxidation temperature, and they could be readily sintered above calcination temperature of 773 K to result in the enhancement of the metal–support interactions. In the case of K_2PtCl_6 precursor, the large hydrogen consumption peak was noticed around 700 K for PtK373 and PtK573 catalysts. The hydrogen consumption peak at a higher temperature implies that it is difficult to be reduced to form the platinum metal-like particles showing high-resistance for chlorine poisoning and also their small interaction with CCl_4 [10,24]. Our previous works [4,5,15,22] suggest that the product distribution was mainly affected by the oxidation states of the various platinum precursors on γ-Al_2O_3 during the steady-state reaction and the

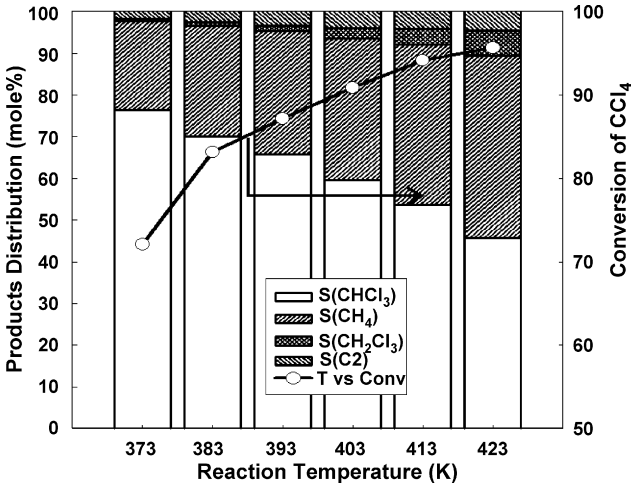

Fig. 1. Effects of reaction temperature on HDC of CCl_4 by using 0.5 wt.% Pt/γ-Al_2O_3 catalyst prepared from $Pt(NH_3)_2(NO_2)_2$. Catalyst (0.5 g) was reduced at 573 K after drying at 373 K. Pg = 0 bar, WHSV = 9000 l/(kg h), H_2/CCl_4 = 9.

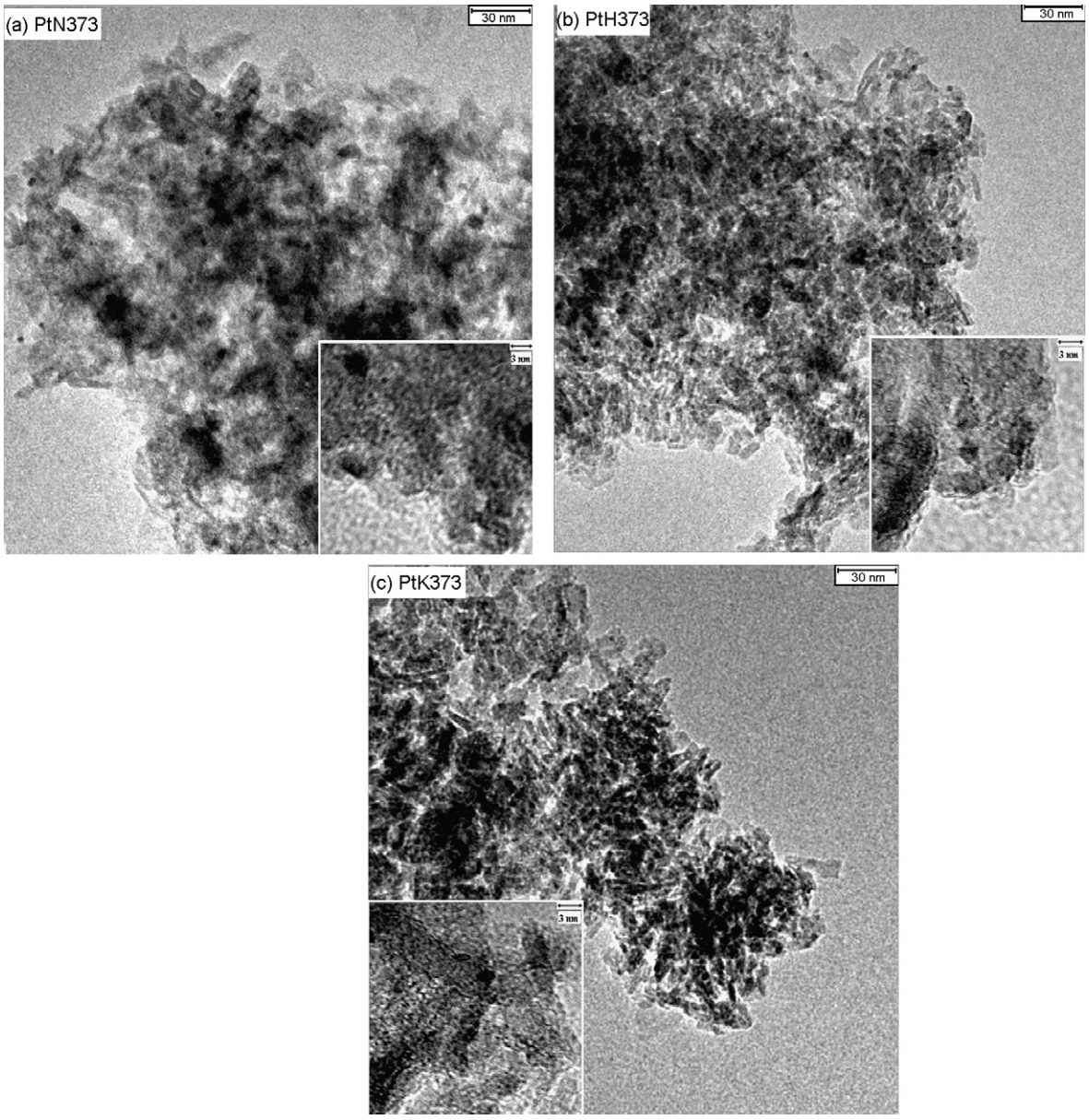

Fig. 2. HRTEM images of 0.5 wt.% Pt/γ-Al_2O_3 catalysts prepared from different platinum precursors after drying at 373 K and reduced at 573 K. (a) PtN373, (b) PtH373 and (c) PtK373.

best selectivity to $CHCl_3$ was obtained for the catalyst possessing an optimum platinum oxidation state. Therefore, the reducibility of platinum particle could also affect the catalytic activity and product distribution by influencing not only desorption properties of products but also the adsorption properties of reactants on the platinum particles [5,7].

3.3. Catalytic activity and product distribution

The conversion and product distribution for the 0.5 wt.% Pt/γ-Al_2O_3 catalysts prepared from $Pt(NH_3)_2(NO_2)_2$, H_2PtCl_6, and K_2PtCl_6 are presented in Tables 2–4. Two typical reaction conditions were employed; a rather mild condition (T = 393 K, P = 0 bar, and mole ratio of H_2/CCl_4 of 9) and a severe condition (T = 413 K, P = 6 bar, and mole ratio of H_2/CCl_4 of 9). Under the mild reaction condition, the mole ratio of $(CHCl_3 + CH_2Cl_2)/CH_4$ increased with the increase of the platinum particle size for all the catalysts prepared from three different platinum precursors. The results suggest that catalysts with larger platinum particle (PtN373) and non-reducible catalysts below 573 K (PtK373 and PtK573) have shown the catalyst deactivation with rather higher selectivity to C_2 compound (mainly C_2Cl_4). However, under the severe reaction conditions, the product distribution showed almost same trend as in the mild reaction conditions. In particular, the generation of CH_2Cl_2 increased for all catalysts. On the catalyst prepared from $Pt(NH_3)_2(NO_2)_2$ precursor, the selectivity to $CHCl_3$ and C_2Cl_4 increased with the concomitant decrease of CH_4 and CH_2Cl_2 formation in both the mild and severe reaction conditions. The catalysts prepared from K_2PtCl_6 also follow the same trend but not changed much in selectivity to $CHCl_3$. For the catalyst prepared from H_2PtCl_6, the selectivity to $CHCl_3$

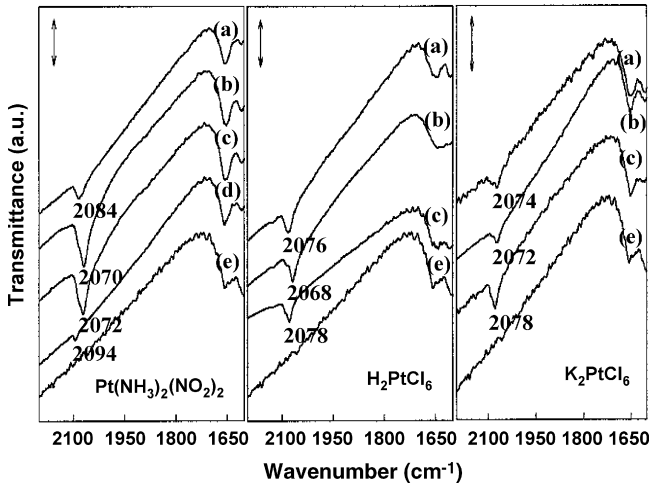

Fig. 3. FT-IR spectra of adsorbed CO on 0.5 wt.% Pt/γ-Al_2O_3 catalysts after calcination at different temperatures and reduction at 573 K. (a) Calcination T = 373 K, (b) calcination T = 573 K, (c) calcination T = 773 K, (d) calcination T = 1073 K and (e) γ-Al_2O_3 support. CO molecules were adsorbed at RT for 1 h and evacuated at the same temperature for 0.5 h.

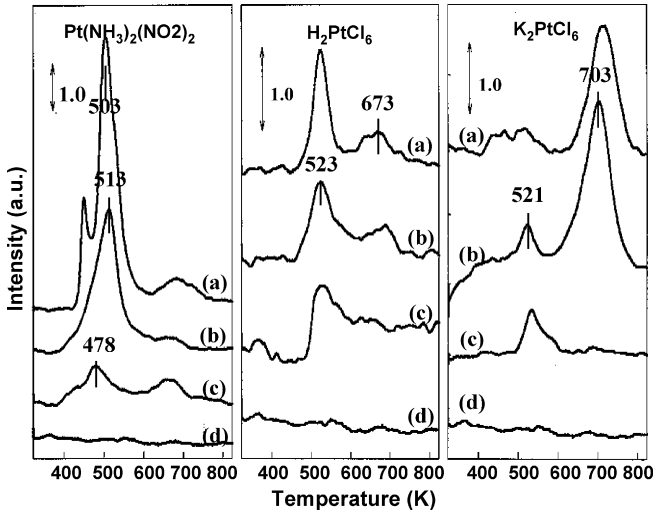

Fig. 4. Temperature-programmed reduction (TPR) profiles on 0.5 wt.% Pt/γ-Al_2O_3 catalysts prepared from different platinum precursors after calcination at different temperatures and reduction at 573 K. (a) Calcination T = 373 K, (b) calcination T = 573 K, (c) calcination T = 773 K and (d) γ-Al_2O_3 support. Catalyst (0.5 g) was analyzed at the following conditions: ramping rate = 10 K/min and flow rate of 5% H_2 balanced with N_2 = 41 μmol/s.

was lower for the catalysts calcined at 573 and 773 K than that for the dried one (PtH373) under the severe reaction condition. Thus, it was irrelevant to platinum particle size. Furthermore, the catalysts treated by a flow of air at 1073 K showed an abrupt deactivation and high selectivity to $CHCl_3$ and C_2Cl_4 at the beginning of reaction. This could be due to the decrease of active sites by severe sintering of platinum particles [26] during the high oxidation treatments, or due to the suppression of the hydrogen activation by severe coke deposition on the relatively large platinum particles at the beginning of reaction. Interestingly, majority of the smaller platinum particles (PtN573 and PtH573) possessing a large electron-deficient character could possibly induce a long retention time of adsorbed CCl_4 resulted in the enhancement of CH_4 formation. Although the products such as $CHCl_3$ and CH_2Cl_2 generated during the HDC reaction could further react with H_2 to form CH_4, the contribution of these effects on product distribution was trivial as mentioned in our previous study [7]. Thus, changes in product distribution are due to the primary reactions of CCl_4, and not due to the secondary reactions of initial products.

3.4. Temperature-programmed desorption (TPD) of CCl_4

TPD analyses of CCl_4 (Table 5) explicitly showed that the amount of adsorbed CCl_4 increased with increasing platinum particle size, although the desorption temperature of CCl_4 on platinum catalysts was almost the same except for Pt573 group. The relative amount of adsorbed CCl_4 ([CCl_4(M)/CCl_4(T)]/dispersion) was normalized by dividing the platinum dispersion [15]. Since CCl_4 was also adsorbed on support itself, the area ratio of CCl_4(M)/CCl_4(T) (area ratio of the desorbed CCl_4 on platinum surface divided by the desorbed CCl_4 on Pt/γ-Al_2O_3 catalyst) could stand for the relative amount of adsorbed CCl_4

Table 2
Conversion and selectivity over 0.5 wt.% Pt/γ-Al_2O_3 prepared from $Pt(NH_3)_2(NO_2)_2$

Catalyst notation	Reaction		Conversion of CCl_4	Selectivity (mole%)				Mole ratio of $(CHCl_3 + CH_2Cl_2)/CH_4$
	T (K)	P (bar)		CH_4	CH_2Cl_2	$CHCl_3$	C_2[a]	
PtN573	393	0	100	36.71	5.03	58.26	0.00	1.724
	413	6	100	54.25	19.40	26.35	0.00	0.843
PtN773	393	0	99.78	20.68	2.55	76.61	0.16	3.828
	413	6	100	22.81	17.20	59.59	0.40	3.367
PtN373[b]	393	0	98.52	16.74	1.38	81.68	0.20	4.962
PtN373	413	6	97.96	22.81	12.25	64.44	0.40	3.362
PtN1073[c]	413	6	92.61	24.52	2.34	72.47	0.67	3.051

Reaction conditions: reduction T = 573 K, WHSV of 4500 l/(kg h), mole ratio of $H_2/CCl_4 = 9 \pm 0.5$ with 0.5 g catalyst. Conversion and selectivity are averaged values measured over 10 h under steady-state reaction conditions.

[a] C_2Cl_4 is the main C_2 compound.

[b] Catalytic deactivation was measured during the HDC reaction.

[c] Conversion and selectivity are obtained after reaction of 10 h.

Table 3
Conversion and selectivity over 0.5 wt.% Pt/γ-Al_2O_3 prepared from H_2PtCl_6

Catalyst notation	Reaction		Conversion of CCl_4	Selectivity (mole%)				Mole ratio of $(CHCl_3 + CH_2Cl_2)/CH_4$
	T (K)	P (bar)		CH_4	CH_2Cl_2	$CHCl_3$	C_2[a]	
PtH573	393	0	100	31.71	3.05	65.24	0.00	2.154
	413	6	100	58.65	32.39	8.96	0.00	0.705
PtH373	393	0	99.98	24.25	1.91	73.70	0.14	3.118
	413	6	99.84	30.06	27.71	42.00	0.23	2.319
PtH773	393	0	99.99	20.30	2.08	77.53	0.09	3.922
	413	6	99.86	46.33	36.20	17.09	0.38	1.150
PtH1073[b]	413	6	88.15	23.09	1.52	74.35	1.04	3.286

Reaction conditions: reduction $T = 573$ K, WHSV of 4500 l/(kg h), mole ratio of $H_2/CCl_4 = 9 \pm 0.5$ with 0.5 g catalyst. Conversion and selectivity are averaged values measured over 10 h under steady-state reaction conditions.
[a] C_2Cl_4 is the main C_2 compound.
[b] Conversion and selectivity are obtained after reaction of 5 h.

Table 4
Conversion and selectivity over 0.5 wt.% Pt/γ-Al_2O_3 prepared from K_2PtCl_6

Catalyst notation	Reaction		Conversion of CCl_4	Selectivity (mole%)				Mole ratio of $(CHCl_3 + CH_2Cl_2)/CH_4$
	T (K)	P (bar)		CH_4	CH_2Cl_2	$CHCl_3$	C_2[a]	
PtK573[b]	393	0	99.36	27.81	1.76	70.37	0.06	2.594
PtK573	413	6	100	31.59	13.99	54.39	0.03	2.165
PtK373[b]	393	0	70.20	12.24	0.28	72.48	15.0	5.944
PtK373	413	6	98.53	29.87	13.30	56.45	0.38	2.335
PtK773	393	0	99.43	19.13	1.28	79.45	0.14	4.220
	413	6	99.76	27.46	17.54	54.81	0.19	2.635
PtK1073[c]	413	6	52.45	18.17	0.53	69.90	11.4	3.876

Reaction conditions: reduction $T = 573$ K, WHSV of 4500 l/(kg h), mole ratio of $H_2/CCl_4 = 9 \pm 0.5$ with 0.5 g catalyst. Conversion and selectivity are averaged values measured over 10 h under steady-state reaction conditions.
[a] C_2Cl_4 is the main C_2 compound.
[b] Catalytic deactivation was measured during the HDC reaction.
[c] Conversion and selectivity are obtained after reaction of 3 h.

Table 5
Temperature-programmed desorption (TPD) analyses of CCl_4

Catalyst notation	Desorption temperature (K)		CCl_4(M)/CCl_4(T)	[CCl_4(M)/CCl_4(T)]/dispersion	Cl/CCl_4(T)
	T_{max} (CCl_4)	T_{dep} (Cl)			
PtN373[a]	381.3	523	0.170	0.491	2.029
PtN573	376.8	633	0.195	0.199	1.076
PtN773	384.6	433	0.137	0.259	4.250
PtN1073[a]	383.1	673	0.185	2.378	0.879
PtH373	386.9	473	0.234	0.406	1.260
PtH573	374.1	475	0.276	0.369	6.950
PtH773	385.7	493	0.168	0.712	1.487
PtH1073[a]	380.2	453	0.201	3.384	4.678
PtK373[a]	383.5	823	0.149	0.350	0.220
PtK573[a]	370.7	673	0.243	0.490	2.951
PtK773	383.1	693	0.171	1.221	0.728
PtK1073[a]	381.9	763	0.146	–	0.353

All catalysts were reduced at 573 K for 3 h with 0.3 g and characterized at the following conditions with GC-MSD 5973; ramping rate = 10 K/min; flow rate (He) = 20.5 μmol/s. CCl_4(M)/CCl_4(T) is the area ratio for the desorbed CCl_4 ($m/z = 117$) on platinum particles (CCl_4(M)) divided by the desorbed CCl_4 on Pt/γ-Al_2O_3 (CCl_4(T)), and Cl/CCl_4(T) is the area ratio of total area of desorbed Cl ($m/z = 36$) divided by CCl_4(T). The maximum desorption temperature of CCl_4 (T_{max}) and the beginning of desorption temperature of Cl_2 or HCl ($m/z = 36$) are also shown.
[a] Deactivation was observed during the HDC reaction at atmospheric reaction pressure.

on platinum surfaces themselves. In our previous studies [7], we have shown the enhanced selectivity to $CHCl_3$ under the optimum pressure with the concomitant increase of total amount of adsorbed CCl_4. The desorption temperature and peak shapes of CCl_4 did not change much to correlate it with adsorption strength of CCl_4, possibly owing to the strongly adsorbed electron-donor (chlorine) or the intra-interaction of adsorbed CCl_4 molecules.

3.5. Characterization of deposited carbonaceous species—TPSR

The carbon deposition on the platinum surfaces could be an important factor for catalyst deactivation and product distribution [7,15,22] as well as platinum particle size. To characterize the carbonaceous species formed at steady-state condition, temperature-programmed surface reaction (TPSR) and FT-IR studies were carried out for the stable catalyst under the following reaction conditions: reduction $T = 573$ K; reaction $T = 413$ K for 5 h; mole ratio of $H_2/CCl_4 = 25$; WHSV = 9000 l/(kg h) with 0.2 g catalyst. Since the deposited carbonaceous species are hard to be removed by hydrogen flow at the reaction conditions, it shows several characteristic peaks appeared at different temperatures. The formation of surface carbons could include surface carbide or amorphous graphite-like carbons. In general, highly multiple-bonded carbons on platinum surface or chlorinated C=C compounds could be removed at higher temperatures to form CH_4 or C_2 hydrocarbons [33]. As shown in Fig. 5, the generation of CH_4 in TPSR experiments showed the three different peak intensities at the characteristic temperature at around 550 K (α), 750 K (β), and 850 K (γ). For the catalysts prepared from $Pt(NH_3)_2(NO_2)_2$ and H_2PtCl_6, the selectivity to CH_4 was enhanced proportionally to the total amount of deposited carbonaceous species. The

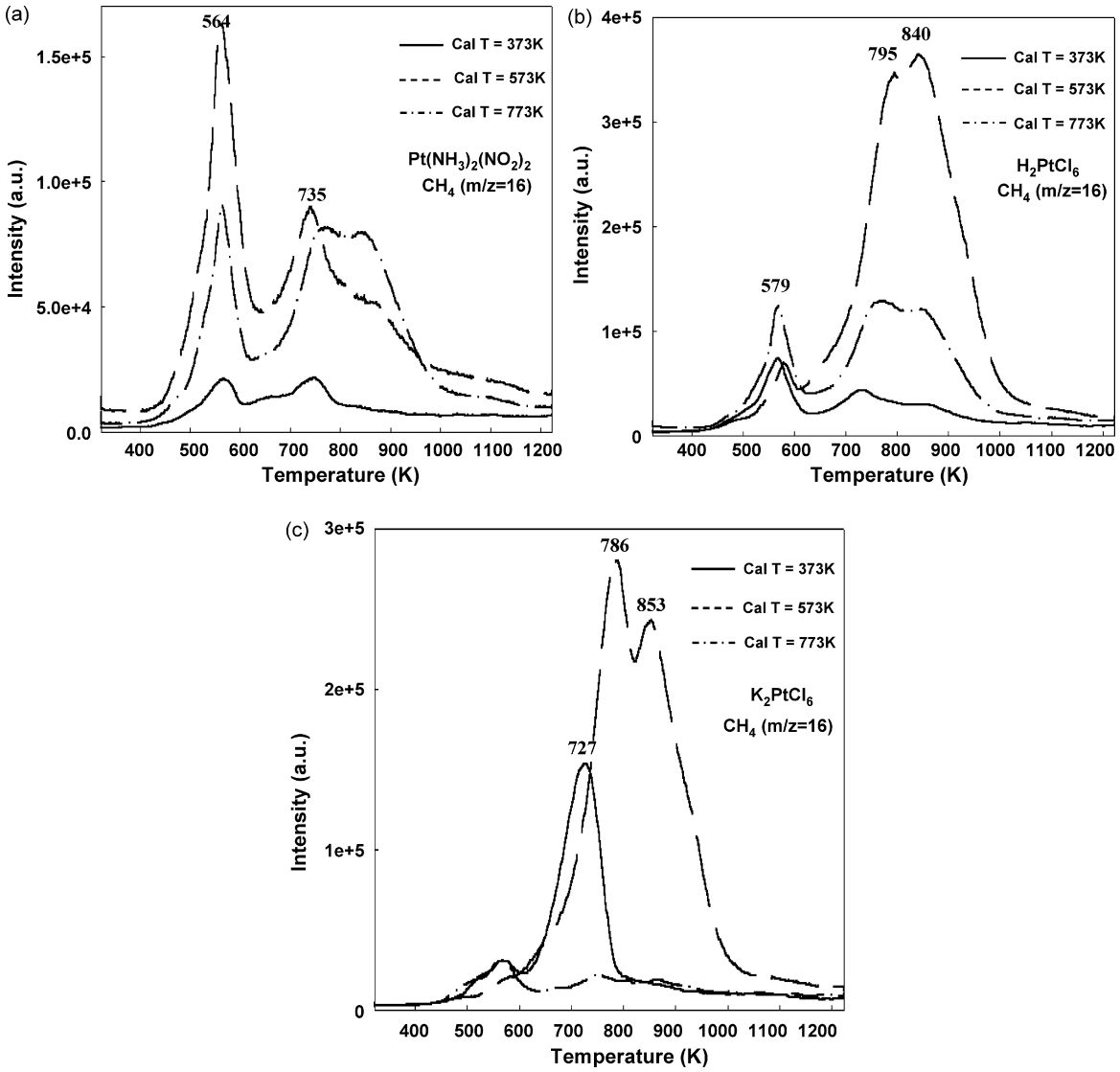

Fig. 5. Temperature-programmed surface reaction (TPSR) on 0.5 wt.% $Pt/\gamma\text{-}Al_2O_3$ catalysts. (a) $Pt(NH_3)_2(NO_2)_2$, (b) H_2PtCl_6 and (c) K_2PtCl_6. (1) Reaction conditions: reduction $T = 573$ K; reaction $T = 413$ K for 5 h, mole ratio of $H_2/CCl_4 = 25$ and WHSV = 4500 l/(kg h) with 0.2 g catalyst. (2) Characterization conditions: ramping rate = 10 K/min and flow rate of H_2 = 20.5 μmol/s. The formed CH_4 ($m/z = 16$) was analyzed by GC-MSD (mass selective detector) 5973.

peak intensities of CH_4 formation (β and γ peaks) are particularly dominant in the catalysts prepared from H_2PtCl_6, whereas α is the main peak for the PtN catalysts. The dried catalysts (PtN373 and PtH373) show the smallest total area of hydrogenated CH_4 and shift to some lower temperature of around 723 K in β peak. The presence of strongly bonded hydrochlorocarbons (β and γ peaks) on the platinum surfaces at the beginning of HDC reaction implies that the deep dechlorination of CCl_4 to form CH_4 could be more favorable on the small sintered platinum particles showing strong metal–support interaction by high oxidation temperatures. Catalysts prepared from K_2PtCl_6 have shown some different TPSR peaks. The high-intensity of β peak appeared at somewhat lower temperature of 727 K for the PtK373 catalyst. It could be due to the non-reducible platinum particles below 573 K (high oxidation states) as shown in Fig. 4 and possibly exist in the form of (un)saturated hydrochlorocarbons. Compared to the PtN and PtH catalysts, the minimum peak intensity was observed in PtK773 catalyst in spite of the large particle size. Interestingly, the total amount of carbonaceous species was much smaller in PtN group than the PtH and PtK group of catalysts. The deposited hydrocarbons concomitantly affect the catalytic activity and product distribution. Furthermore, they were enhanced in some platinum particles showing high electron-deficient characters due to the intrinsic platinum precursor effects, especially in the chlorine-containing H_2PtCl_6 and K_2PtCl_6 ones, as mentioned earlier [5], or the intrinsic small platinum effects and non-reducible particles below 573 K to possess the high oxidation states.

3.6. Characterization of deposited carbonaceous species—infrared studies

To further identify the deposited carbonaceous species during HDC, FT-IR studies (Fig. 6) were carried out at the same reaction conditions as in TPSR studies. Some authors have assigned the adsorbed chlorinated carbons on the catalyst surfaces using in situ FT-IR techniques [35,36]. Greene and Chintawar [35] reported that the separately adsobed vinyl chloride (VC, $H_2C{=}CHCl$) or trichloroethylene (TCE, $HClC{=}CCl_2$) on Cr–Y zeolite showed a distinct band at 1604 cm^{-1} for C=C stretching mode and 1387 cm^{-1} for CH_2 deformation, C–H rock band at 1269 cm^{-1} for VC and CH–Cl bending band at 1254 cm^{-1} for TCE. Hindermann and coworkers [36] have shown that the FT-IR spectra of bending frequency of CH_2Cl_2 adsorbed on γ-Al_2O_3 appeared at the frequency of 1279 and 1268 cm^{-1} and assigned the band at 1468 and 1420 cm^{-1} for the asymmetric bending modes of surface methoxy groups. Furthermore, the broad peaks around 1350–1640 cm^{-1} could be assigned to be carboxylate or acetate species formed on Al_2O_3 surfaces by the adsorption of chlorinated C_2 compounds [35,36] and the sharp peak at 1266 cm^{-1} to C–H rock/CH–Cl bending vibration on the surfaces of Al_2O_3 or platinum particles. Trombetta et al. [37] showed the IR band position of butenes and propene on γ-Al_2O_3 during the skeletal isomerization of *n*-butene to isobutene. For all butenes and propene bands below 1500–1250 cm^{-1} were assigned to the C–H deformation (–CH_2 or –CH_3) and C–C stretching vibration.

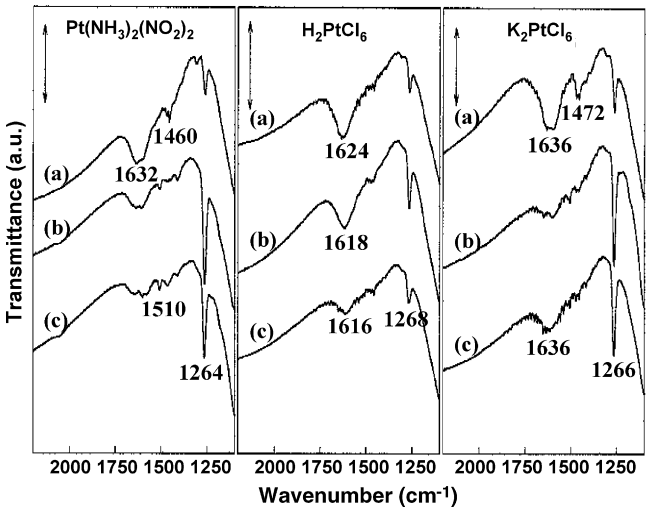

Fig. 6. FT-IR spectra of various 0.5 wt.% Pt/γ-Al_2O_3 catalysts after HDC of CCl_4: (a) 0.5 wt.% Pt/γ-Al_2O_3, calcination T = 373 K, reduction T = 573 K; (b) 0.5 wt.% Pt/γ-Al_2O_3, calcination T = 573 K, reduction T = 573 K; (c) 0.5 wt.% Pt/γ-Al_2O_3, calcination T = 773 K, reduction T = 573 K. The sample used for HDC reaction for 5 h was evacuated at room temperature under high-vacuum system for 1 h. Reaction conditions: reduction T = 573 K, reaction T = 413 K, mole ratio of H_2/CCl_4 = 25 and WHSV = 9000 l/(kg h).

The FT-IR spectra for stable catalysts shown in Fig. 6 suggest that the bands appeared with relatively lower intensity in the regions of 1575–1630 cm^{-1} and higher one at around 1266 cm^{-1} for PtN573 and PtN773. But, for PtN373, the intensity of the band at 1266 cm^{-1} was diminished due to the small amount of carbon deposition. The results of TPSR and FT-IR suggest that the carbonaceous species on the calcined PtN catalysts are mainly in the deep dechlorinated hydrocarbons such as mainly CH_xCl_y. Furthermore, the intensity at the frequency of 1264 cm^{-1} is proportional to that of α peak in TPSR. The high-intensity peaks around 1575–1630 cm^{-1} and a low-intensity peak at 1264 cm^{-1} for PtH catalyst suggest that the main carbonaceous species formed on the platinum surface are possibly in the form of deep dechlorinated amorphous graphite-like carbons like β and γ peaks in TPSR. For the PtK group, $C_2H_xCl_y$ including C_2Cl_4 and C_2Cl_6 that has much higher boiling point than reaction temperature, could be the main carbonaceous species and responsible for high peak intensity at 1266 cm^{-1}. The selectivity to C_2 and the catalyst deactivation was enhanced due to the formation of these intermediates. From the FT-IR and TPSR results of stable catalysts at the beginning of reaction, the carbonaceous species are much smaller on the catalysts dried at 373 K, without calcinations, than the others.

But, the initially formed carbonaceous species are further progressed to the more inactive ones such as γ form as reaction time increased up to 55–70 h in all catalysts (Fig. 7). Interestingly, Pt373 group showed much enhanced carbon deposition in spite of the small amount carbon depositon at the beginning of reaction. Although these catalysts showed high selectivity to $CHCl_3$, deactivation rates were somewhat higher

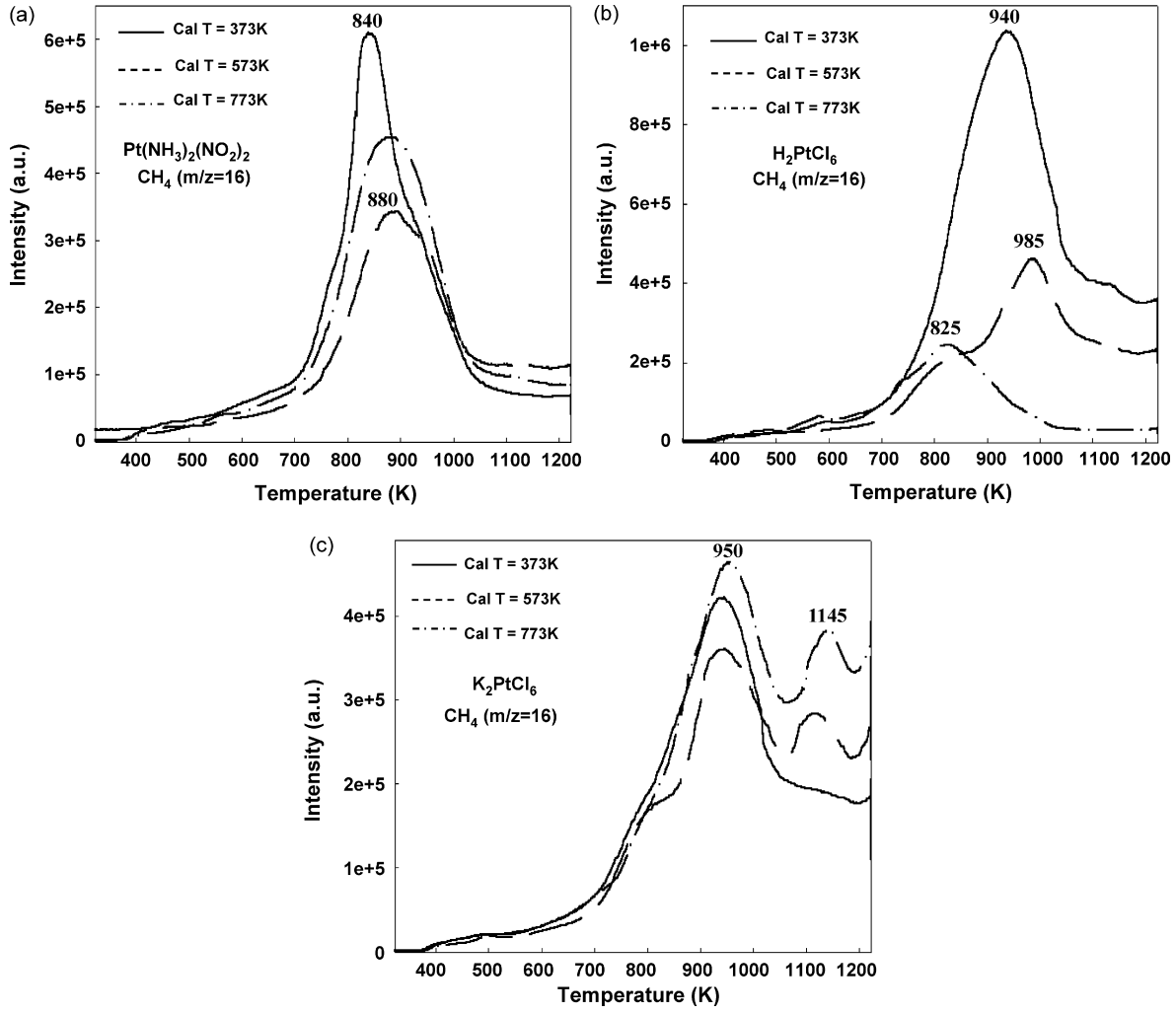

Fig. 7. Temperature-programmed surface reaction (TPSR) of 0.5 wt.% Pt/γ-Al_2O_3 catalysts prepared from different platinum precursors. (a) $Pt(NH_3)_2(NO_2)_2$, (b) H_2PtCl_6 and (c) K_2PtCl_6. (1) Reaction conditions: reduction T = 573 K, reaction T = 393–413 K for 55 h–70 h, reaction Pg = 0–6 bar, mole ratio of $H_2/CCl_4 = 9 \pm 0.5$ and WHSV = 4500 l/(kg h) with 0.5 g catalyst. (2) Characterization conditions: ramping rate = 10 K/min and flow rate of H_2 = 20.5 μmol/s with 0.2 g. The formed CH_4 (m/z = 16) was analyzed by GC-MSD (mass selective detector) 5973.

than the other calcined catalysts. The progressively transformed carbons from α to γ form with time on stream could be the main factor for the catalyst deactivation and cause the changes in product distribution.

4. Discussion

The effects of metal particle size on the catalyst stability have been reported previously by several researchers [6,10,22]. However, the correlation of product distribution in HDC of CCl_4 with platinum particle size on catalysts prepared from various platinum precursors at different calcination temperatures has not been studied so far. In the study of structure-sensitivity for hydrogenolysis of C-halogen compounds, some authors proposed that large particles above 5–8 nm in diameter had almost the same electronic character like a bulk metal, and they could be proposed as the active and selective sites for HDC [10,32]. In our previous studies [5,7,15,22], we have shown that the change of product distribution in HDC of CCl_4 on Pt/γ-Al_2O_3 was explained as a function of electronic effects of platinum particles and a relative amount of adsorbed reactants. The vacancy of the incomplete d-band of the surface platinum particles prepared from different platinum precursors was correlated with the adsorption strength of reactants or products. Furthermore, the optimum coverage of reactants such as H_2 and CCl_4 competitively adsorbed on the platinum particles had an effect on the product distribution. As the metal particle size increases, the local density of states (LDS) at the Fermi level could increase (decrease in oxidation states of platinum particles) and change the interaction of CCl_4 with platinum particles.

As shown in Table 1 and Figs. 2–4, the prepared catalysts exhibited different platinum particle size depending on the calcination temperatures and the platinum precursors employed during the preparation. The electronic states and morphology of platinum particles could be also altered according to platinum particle size. The dried catalysts without calcination (Pt373 group) were redispersed by calcination at 573 K to form a small platinum particle size. However, they are sintered at calcination above 773 K according to the well-known sintering process. The

mobile platinum species on the support could be more easily formed in the chloride-containing precursors such as H_2PtCl_6 and K_2PtCl_6 [10,13,14,16] and resulted in varying the metal dispersion and also the metal–support interaction. The interaction of supported metal with the linear-bonded CO molecule are explained by the morphology of metal particles as well as the electron transfer from metal to $2\pi^*$ orbital of CO by electron back-donation resulted to weaken the C–O bond and shift the CO absorption bands to lower frequencies. Some authors reported that the frequency of the stretching mode of linear-bonded CO increased with increasing the metal particle size. Furthermore, CO frequency associated with the edge and corner sites are lower than that of face sites [10,13,25,31]. The more coordinatively saturated the metal atoms (high coordination number of metal atoms), the higher will it be the frequency of CO absorption bands. As shown in Fig. 3, the maximum peak position of linear-bonded CO frequency shifted to the higher frequency with increasing platinum particle size in all our catalysts. TPR results (Fig. 4) suggest that the reducibility of platinum particles was observed in the following order; PtN > PtH ≫ PtK. The peak around 700 K in TPR could be assigned due to the reduction of metal oxide strongly interacting with the support, and its intensity were found to be relatively larger for PtK catalysts than for PtN and PtH catalysts. As reported in our previous works [5–7,22], the catalyst stability and selectivity to $CHCl_3$ in HDC were enhanced with the large platinum particles showing more metallic character and with a lower oxidation states. It could be induced by the changes in adsorption/desorption character of intermediates and the relative amounts of competitively adsorbed hydrogen and CCl_4 on the platinum particles as well [7,22].

The product distribution (Tables 2–4) clearly suggests that a good correlation is obtained with platinum particles size under the mild reaction conditions (T = 393 K, P = 0 bar, and mole ratio of H_2/CCl_4 of 9). In the pressurized reaction conditions, the selectivity to $CHCl_3$ and catalysts stability was also increased with increase of platinum particle size for all the studied catalysts. Furthermore, the normalized amount of adsorbed CCl_4 increased with increase of platinum particle size as reported in Table 5 (TPD analyses). The catalysts showing relatively high amount of adsorbed CCl_4 (PtN1073, PtH1073, and PtK1073) and non-reducibility below 573 K such as PtK373 and PtK573 were rapidly deactivated with a concomitant generation of C_2Cl_4. In the severe reaction conditions (T = 413 K, P = 6 bar, and mole ratio of H_2/CCl_4 of 9), these trends were distorted significantly, especially for PtH catalyst. As mentioned earlier by XANES analyses [5], the relatively high adsorption strength of CCl_4 in the PtH group could be the reason for the higher selectivity to CH_4 and CH_2Cl_2. It could be from the intrinsic character of small platinum particle size or strong metal–support interactions of PtH group. At the high reaction temperature (413 K) and pressure (6 bar), the C–Cl bond dissociation could be more favorable to form more highly dechlorinated products such as CH_2Cl_2, CH_3Cl, and CH_4 with the increased rate of hydrogen activation on platinum surfaces. These phenomena were more favorable on the electron-deficient small platinum particles. If the low electron density of d-orbital is the character of small platinum particles, the selectivity to deep-dechlorinated CH_4 could increase due to the strong adsorption strength of CCl_4 and the large amount of activated hydrogen (low hydrogen activation energy) [5,7,38]. Therefore, the production of CH_2Cl_2 and CH_4 were more prominent in PtN573, PtH573, and PtH373. These trends were summarized in Fig. 8a and b in terms of $(CHCl_3 + CH_2Cl_2)/CH_4$ mole ratio and the maximum peak position of linear-bonded CO.

As the adsorption strength of CCl_4 increases on the platinum surfaces, the propensity to surface carbon formation also increases, especially in Pt373K group (Fig. 7), resulting in the enhancement of CH_4 selectivity. The γ peak in TPSR shown in Figs. 5 and 6 increased with decrease of platinum particle size in the PtN and PtH catalysts. However, the total amounts of observed carbonaceous species are found to be much lower for Pt373 group than that for Pt573 and Pt773 groups except for PtK catalysts at the beginning of the reaction. In PtN group

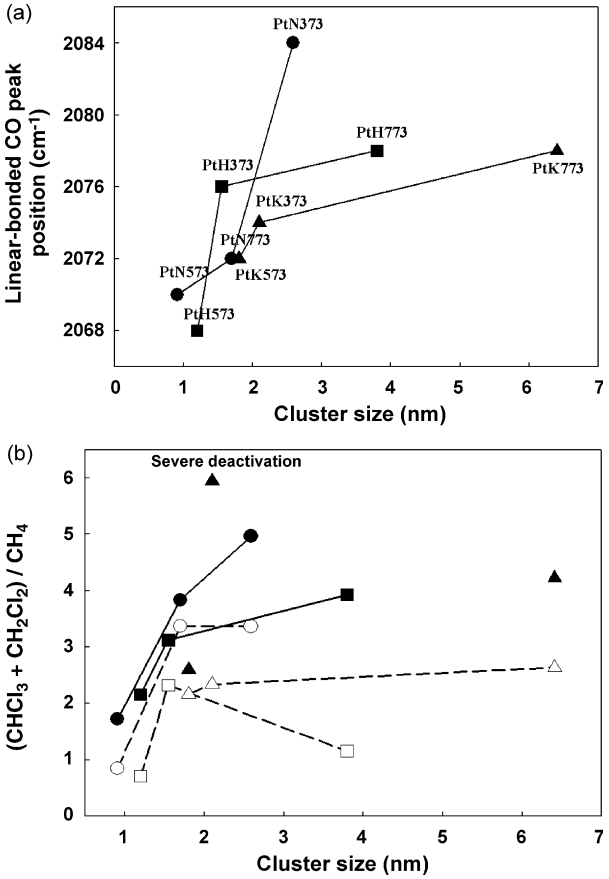

Fig. 8. Effects of platinum cluster size on the band positions of the linear-bonded CO in FT-IR and products distribution ($[CHCl_3 + CH_2Cl_2]/CH_4$). (a) Platinum cluster size vs. linear-bonded CO peak position and (b) platinum cluster size vs. product distribution ($[CHCl_3 + CH_2Cl_2]/CH_4$). (●) 0.5 wt.% Pt/γ-Al_2O_3, $Pt(NH_3)_2(NO_2)$.(■) 0.5 wt.% Pt/γ-Al_2O_3, H_2PtCl_6. (▲) 0.5 wt.% Pt/γ-Al_2O_3, K_2PtCl_6. The filled points: product mole ratio of $(CHCl_3 + CH_2Cl_2)/CH_4$ at mild reaction conditions: T = 393 K, P = 0 bar, mole ratio of H_2/CCl_4 of 9 ± 0.5. The blank points: product mole ratio of $(CHCl_3 + CH_2Cl_2)/CH_4$ at severe reaction conditions: T = 413 K, P = 6 bar, mole ratio of H_2/CCl_4 of 9 ± 0.5.

catalysts, as the platinum particle size decrease, the total carbonaceous species and the relatively high band intensity at 1264 cm^{-1} at FT-IR (Fig. 6) increased with further increase of CH_4 selectivity. It could be due to the intrinsic electron-deficient character of small platinum particles to enhance the adsorption strength of CCl_4 and more selectively form CH_4 as well as carbonaceous species. For PtH catalyst, the β and γ peaks in TPSR were much higher in the calcined catalysts (PtH573 and PtH773) than that of dried one (PtH373). These peaks could be assigned to the strongly adsorbed intermediates due to the high electron-deficient character and resulted in the enhanced selectivity to CH_4. The PtK catalysts are difficult to be reduced below 573K (PtK373 and PtK573) with hydrogen (Fig. 4) resulted in enhancing the adsorption strength of reactants and intermediates. Therefore, the formation of C_2 compounds and catalyst deactivation was enhanced. All the catalysts prepared from different platinum precursors and calcined at different temperatures have shown the enhancement of selectivity to $CHCl_3$ with increasing platinum particle size under the mild reaction conditions. The changes in product distribution are related with the intrinsic electronic state of platinum particles which are also modified by different calcination temperatures and the platinum precursors. The catalyst deactivation was mainly due to the progressive transformation of carbonaceous species from α to γ, and the amount of deposited carbons at the beginning of reaction also affected the product distribution.

5. Conclusions

TP methods (TPR, TPD and TPSR), FT-IR, HRTEM and CO chemisorption were carried out to find the effect of platinum particle size according to the different platinum precursors on the product distribution. The platinum particle size was affected by the different thermal treatments of 0.5 wt.% Pt on γ-Al_2O_3. Product distribution and catalytic stability were also altered depending on the platinum particle size. In our reaction conditions, the small platinum particles, which are related to the low coordination number and electron-deficient properties, induced a more favorable deep HDC of CCl_4 to form the completely dechlorinated CH_4. It could be due to the long residence time of CCl_4 and relatively low activation energy of hydrogen on the small platinum particles. TPSR and FT-IR studies for stable catalysts showed characteristic carbonaceous species on the prepared catalysts. The amount of the carbonaceous species such as CH_xCl_y and chlorinated C=C compounds, decreases on the large platinum surfaces and the selectivity to $CHCl_3$ was enhanced. The larger the platinum particle sizes, the higher selectivity to $CHCl_3$ was obtained under the mild reaction conditions.

References

[1] A.H. Weiss, B.S. Gambhir, R.B. Leon, J. Catal. 22 (1971) 245.
[2] A.H. Weiss, S. Valinski, G.V. Autolsin, J. Catal. 74 (1982) 136.
[3] S.Y. Kim, H.C. Choi, O.B. Yang, K.H. Lee, J.S. Lee, Y.G. Kim, J. Chem. Soc., Chem. Commun. (1995) 2169.
[4] H.C. Choi, S.H. Choi, J.S. Lee, K.H. Lee, Y.G. Kim, J. Catal. 161 (1996) 790.
[5] H.C. Choi, S.H. Choi, J.S. Lee, K.H. Lee, Y.G. Kim, J. Catal. 166 (1997) 284.
[6] Z.C. Zhang, B.C. Beard, Appl. Catal. A: Gen. 174 (1998) 33.
[7] J.W. Bae, E.D. Park, J.S. Lee, K.H. Lee, Y.G. Kim, S.H. Yeon, B.H. Sung, Appl. Catal. A: Gen. 217 (2001) 79.
[8] X. Wu, Y.A. Letuchy, D.P. Eyman, J. Catal. 161 (1996) 164.
[9] B. Coq, F. Figueras, Coord. Chem. Rev. 178–180 (1998) 1753.
[10] Z.C. Zhang, B.C. Beard, Appl. Catal. A: Gen. 188 (1999) 229.
[11] J. Okal, H. Kubicka, Appl. Catal. A: Gen. 171 (1998) 351.
[12] G.J. Arteaga, J.A. Anderson, C.H. Rochester, J. Catal. 184 (1999) 268.
[13] M.G.V. Mordente, C.H. Rochester, J. Chem. Soc., Faraday Trans. 1 85 (10) (1989) 3495.
[14] G. Lietz, H. Lieske, H. Spindler, W. Hanke, J. Volter, J. Catal. 81 (1983) 17.
[15] J.W. Bae, E.J. Jang, B.I. Lee, J.S. Lee, K.H. Lee, Ind. Eng. Chem. Res. 46 (2007) 1721.
[16] T.J. Lee, Y.G. Kim, J. Catal. 90 (1984) 279.
[17] S. Balcon, S. Mary, C. Kappenstein, E. Gengembre, Appl. Catal. A: Gen. 196 (2000) 179.
[18] B. Coq, G. Ferrat, F. Figueras, J. Catal. 101 (1986) 434.
[19] J.W. Bozzelli, Y.M. Chen, Chem. Eng. Commun. 115 (1992) 1.
[20] M. Martino, R. Rosal, H. Sastre, F.V. Diez, Appl. Catal. B: Environ. 20 (1999) 301.
[21] E.J. Creyghton, M.H.W. Byrgers, J.C. Jansen, H. van Bekkum, Appl. Catal. A: Gen. 128 (1995) 275.
[22] J.W. Bae, I.G. Kim, J.S. Lee, K.H. Lee, E.J. Jang, Appl. Catal. A: Gen. 240 (2003) 129.
[23] G. Jacobs, F. Ghadiali, A. Pisanu, A. Borgna, W.E. Alvarez, D.E. Resasco, Appl. Catal. A: Gen. 188 (1999) 79.
[24] P.V. Menacherry, G.L. Haller, J. Catal. 177 (1998) 175.
[25] M.J. Kappers, J.H. van der Maas, Catal. Lett. 10 (1991) 365.
[26] M.R. Othman, N.N.N. Mustafa, A.L. Ahmad, Micropor. Mesopor. Mater. 91 (2006) 268.
[27] J. Llorca, N. Homs, J. Leon, J. Sales, J.L.G. Fierro, P. Ramirez de la Piscina, Appl. Catal. A: Gen. 189 (1999) 77.
[28] M. Pauris, H. Peyrard, M. Montes, J. Catal. 199 (2001) 30.
[29] G. Blyholder, J. Phys. Chem. 68 (10) (1964) 2772.
[30] K.A. Frankel, B.W.L. Jang, J.J. Spivey, G.W. Roberts, Appl. Catal. A: Gen. 205 (2001) 263.
[31] R.G. Greenler, K.D. Burch, K. Kretzschmar, R. Klauser, A.M. Bradshaw, Surf. Sci. 152–153 (1985) 338.
[32] W.M.H. Sachtler, A.Yu. Stakheev, Catal. Today 12 (1992) 283.
[33] R.E. Hayes, K.J. Ward, K.E. Hayes, Appl. Catal. 20 (1986) 123.
[34] Z. Hlavathy, P. Tetenyi, Surf. Sci. 410 (1998) 39.
[35] P.S. Chintawar, H.L. Greene, J. Catal. 165 (1997) 12.
[36] R.W. van den Brink, P. Mulder, R. Louw, G. Sinquin, C. Petit, J.P. Hindermann, J. Catal. 180 (1998) 153.
[37] M. Trombetta, G. Busca, S.A. Rossini, R. Picoli, U. Cornaro, J. Catal. 168 (1997) 334.
[38] M.T. Paffett, S.C. Gebhard, R.G. Windham, B.E. Koel, J. Phys. Chem. 94 (1990) 6831.